Mon. Not. R. Astron. Soc. **000**, 1–?? (2013) Printed 3 February 2017 (MN LATEX style file v2.2)

The dusty aftermath of SN Hunt 248: merger-burst remnant?

Jon C. Mauerhan[1⋆], Schuyler D. Van Dyk[2], Joel Johansson[3], Ori D. Fox[4], Alexei V. Filippenko[1], Melissa L. Graham[5,1]

[1] *Department of Astronomy, University of California, Berkeley, CA 94720-3411, USA*
[2] *Infrared Processing and Analysis Center, California Institute of Technology, Pasadena, CA 91125, USA*
[3] *Department of Particle Physics and Astrophysics, Weizmann Institute of Science, 234 Herzl St., Rehovot, Israel*
[4] *Space Telescope Science Institute, 3700 San Martin Drive, Baltimore, MD 21218, USA*
[5] *Department of Astronomy, University of Washington, Box 351580, Seattle, WA 98195-1580*

arXiv:1702.00430v1 [astro-ph.SR] 1 Feb 2017

3 February 2017

ABSTRACT

Supernova SN Hunt 248 was classified as a nonterminal eruption (a SN "impostor") from a directly identified cool hypergiant star. The transient achieved peak luminosity equivalent to that of η Car's historic outburst and exhibited a multi-peaked optical light curve that rapidly faded after ~ 100 days. We report ultraviolet (UV) through optical observations of SN Hunt 248 with the *Hubble Space Telescope (HST)* ~ 1 yr after the outburst, and mid-infrared observations with the *Spitzer Space Telescope* before the burst and in decline. The *HST* data reveal a source that is a factor of ~ 10 fainter in the optical than the faintest available measurement of the precursor star, yet exhibits the same $B-V$ colour. Substantial mid-infrared excess of the source is consistent with thermal emission from newly synthesized hot dust, possibly heated by a surviving star. However, the lack of substantial reddening of the UV-optical source appears inconsistent with substantial absorption of the stellar light; possible explanations for the discrepancy include UV-optical contamination from a neighbouring star, or inefficient dust absorption, perhaps the result of an aspherical dust distribution. Reanalysis of the earlier outburst data shows that the peak luminosity and outflow velocity of the eruption are consistent with a trend exhibited by stellar merger candidates. Alternatively, if SN Hunt 248 marked the genuine death of a massive star from a weak explosion or failed SN, then the late-time photometry suggests that $\lesssim 6.5 \times 10^{-4}\,\mathrm{M}_{\odot}$ of radioactive ^{56}Ni was synthesized. Future space-based monitoring of the UV-infrared counterpart is necessary to elucidate the nature of the source, the outburst, and the uncertain fate of the culprit star.

Key words: supernovae: general — supernovae: individual (SN Hunt 248)

1 INTRODUCTION

SN impostors (Van Dyk et al. 2000) are violent nonterminal outbursts from evolved massive stars, akin to the historic outbursts of Galactic luminous blue variable (LBV) stars η Car and P Cygni. The physical mechanisms responsible for the outbursts and their associated mass ejections are poorly understood and mostly unaccounted for in stellar evolution models (see Smith 2014 for a review). Current possibilities include instabilities associated with late-stage nuclear burning (Shiode & Quataert 2014; Smith & Arnett 2014), violent binary encounters (Smith & Frew 2011), and even stellar mergers involving massive binary star systems (Smith et al. 2016; Kochanek et al. 2014a).

Recent studies of the fading optical-infrared (IR) remnants of luminous transient have shown that objects previously classified as SN impostors might actually be terminal explosions after all, in which a stellar core collapses, but with an incomplete or failed expulsion of the stellar mantle. Indeed, the fate of the prototype impostor SN 1997bs has recently come under question, based on the unexpectedly low luminosity for the optical-IR remnant relative to the directly identified stellar precursor (Adams & Kochanek 2015). The fate of other historic transients for which high-quality precursory data were not available have also been the source of ongoing debate (e.g., SN 1961V; Smith et al. 2011; Van Dyk et al. 2013), in part because persistent line

⋆ E-mail: mauerhan@astro.berkeley.edu

© 2013 RAS

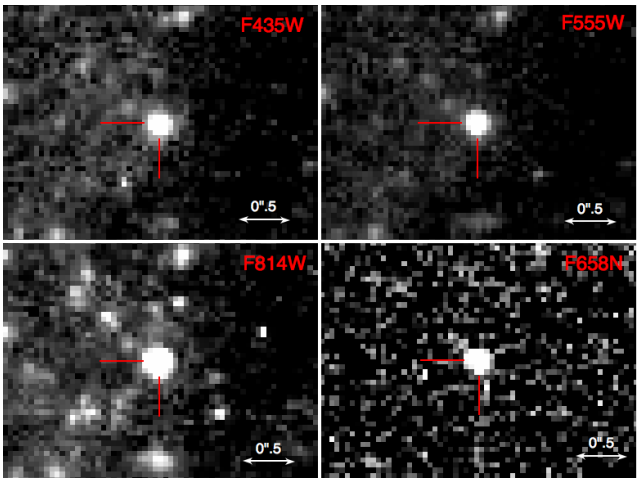

Figure 1. *HST*/WFPC2 and ACIS images (log stretch) of the cool-hypergiant precursor of SN Hunt 248 (see Mauerhan et al. 2015), from 3374 days before the onset of the 2014 eruption (broad-band filter images; the F658N image is from 3715 days before eruption). North is up and east is toward the left.

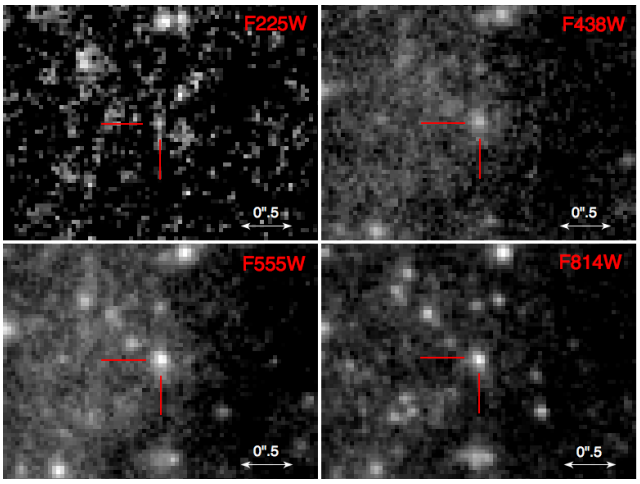

Figure 2. *HST*/WFC3 images (log stretch) of the remnant of SN Hunt 248, ∼386 days after the onset of the 2014 eruption. North is up and east is toward the left.

emission detected at the sites might be the result of ongoing interaction between the explosion and extended circumstellar material (CSM) rather than emission from a surviving star.

SN Hunt 248 was a luminous transient in NGC 5806 classified as a SN "impostor. The light curve exhibited a main peak equivalent in luminosity to the peak of η Car's historic outburst in the 1840's, and another subsequent peak of longer duration that was likely the result of interaction with pre-existing CSM expelled prior to the outburst (Mauerhan et al. 2015). A particularly interesting aspect of SN Hunt 248 is the detection of the luminous precursor star in archival data, shown in Figure 1 (Mauerhan et al. 2015). Multi-colour photometry from the *Hubble Space Telescope (HST)* showed that the stellar precursor's position on the Hertzsprung-Russell (HR) diagram was consistent with a cool hypergiant star. The subsequent giant eruption from the star in 2014 provided observational support for a hypothesis that cool hypergiants might actually be relatively hot LBV stars enshrouded in an opaque wind that creates an extended pseudo-photosphere (Smith & Vink 2009). Detailed study of the aftermath of the eruption thus provides an interesting opportunity to probe the post-outburst state and recover the stellar remnant.

Here we present ultraviolet (UV) through IR observations of SN Hunt 248 with the *HST* and the *Spitzer Space Telescope* ~ 1 yr after the giant outburst. The times of all observation epochs are presented as days past V-band peak on UT 2014 June 21 (MJD 56830.3). A foreground extinction value of $A_V = 0.14$ mag has been adopted (Mauerhan et al. 2015).

Table 1. *HST* photometry of the remnant of SN Hunt 248.

Instrument/Band	Magnitude	Flux (μJy)	MJD	Epoch (days)
WFC3/F225W	25.16 ± 0.09	0.068 ± 0.006	57204.05	374
WFC3/F438W	25.84 ± 0.05	0.193 ± 0.010	57204.00	374
WFC3/F555W	25.46 ± 0.03	0.243 ± 0.007	57199.87	370
ACS/F814W	24.51 ± 0.04	0.386 ± 0.015	57200.38	371

[a]Uncertainties are statistical. Epochs are given as days from V-band peak (MJD 56830.3; Mauerhan et al. 2015).

2 OBSERVATIONS

2.1 *HST* Imaging

High-resolution imaging observations of SN Hunt 248 were performed with the *HST* Wide-field Camera 3 (*HST*/WFC3) on 2015 June 26 and 30 (days 369 and 374 days after the peak of the 2014 eruption) under *HST* programs GO-13684 and GO-13822 (PIs S. Van Dyk and G. Folatelli, respectively). Exposures were obtained in the F225W (NUV), F438W (B), F555W (V), and F814W (I) filters. A point source at the position of SN Hunt 248 is securely detected in all bands, as shown in Figure 2. Photometry of the source was extracted from the images using Dolphot (Dolphin 2000). We tried two different approaches to estimate the background, including the use of an annulus region to measure the sky (FitSky=1) and, alternatively, measuring the sky within the point-spread function PSF aperture (FitSky=3, best to use when the field is very crowded). Our annulus-based background subtraction produced the most consistent results for all bands, although the results from each setting are within the respective uncertainties. The photometry is listed in Table 1.

2.2 *Spitzer* Imaging

SN Hunt 248 was observed on five epochs during the *Spitzer Space Telescope* Warm Mission utilizing channels 1 (3.6 μm) and 2 (4.5 μm) of the Infrared Array Camera (IRAC; Fazio et al. 2004). We acquired fully coadded and calibrated data from the *Spitzer* Heritage Archive[1] from program IDs 61063 (PI K. Sheth), 10152 (PI M. Kasliwal), and 11053 (PI O.

[1] http://sha.ipac.caltech.edu/applications/Spitzer/SHA/

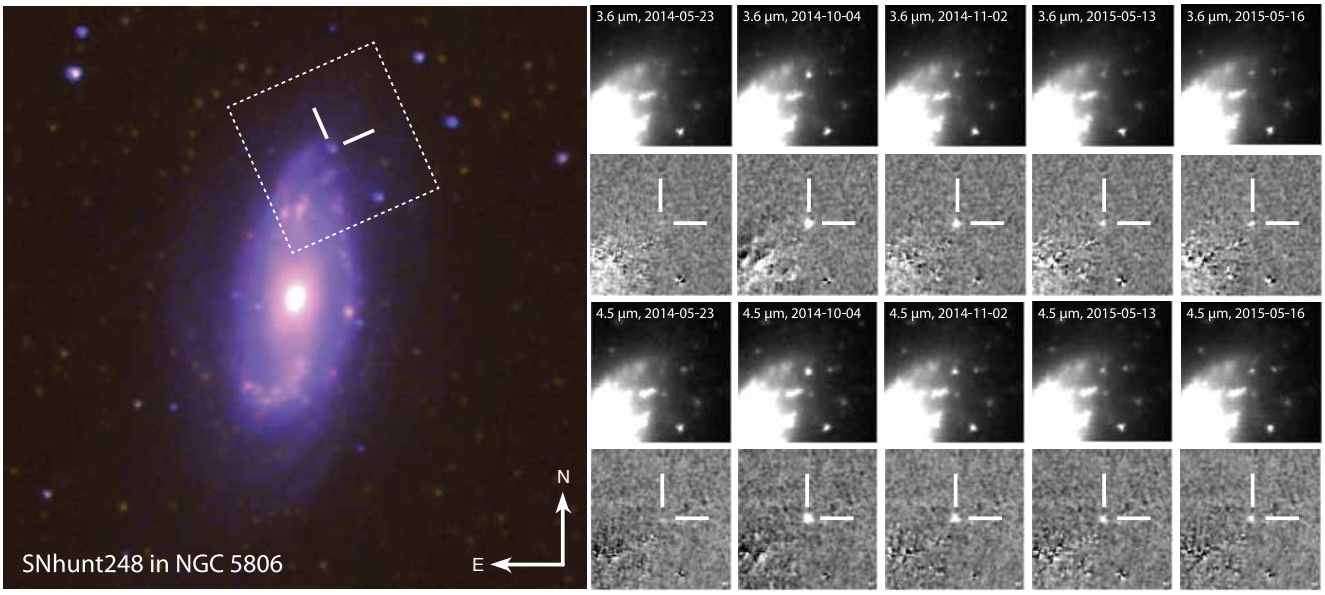

Figure 3. Colour composite of the 3.6 μm (green) and 4.5 μm (red) *Spitzer*/IRAC template images of NGC 5806 and a Palomar Transient Factory R-band image (blue), and the template-subtracted images of the region around SN Hunt 248 (tiled frames).

Fox). The images for all epochs were registered with an earlier pre-outburst image of the host galaxy, which was used as a subtraction template. The template-subtracted images are shown in Figure 3. We performed aperture photometry on the template-subtracted (PBCD / Level 2) images using a 6-pixel aperture radius and aperture corrections listed in Table 4.7 of the *Spitzer* IRAC Instrument Handbook[2]. The background and noise levels in the subtracted images were computed from 100 randomly placed apertures near the source location. Upper limits for the source from the template image were obtained from the same 6-pixel aperture, after subtracting the average flux within 8 background apertures of equal size at 12 pixel distances from the source position and adding the upper bound of the standard deviation within those apertures. The photometry results are listed in Table 2. The observational coverage ranged from -1763 days to $+328$ days with respect to optical peak of the outburst (Mauerhan et al. 2015). The earliest mid-IR detection of the source was at -30 days from peak of the main outburst, which was ~ 2 weeks before the onset of the outburst.

Table 2. *Spitzer*/IRAC photometry of SN Hunt 248.

MJD	Epoch (days)	3.6 μm	4.5 μm	Program ID (PI)
55066.9	-1763	< 9.49	< 5.99	61063 (Sheth)
56800.7	-30	19.35 ± 6.11	11.81 ± 5.09	10152 (Kasliwal)
56934.6	104	110.26 ± 6.38	96.41 ± 5.86	10152 (Kasliwal)
56963.4	133	65.56 ± 6.14	59.70 ± 5.91	10139 (Fox)
57155.5	325	32.72 ± 7.82	29.26 ± 4.76	11053 (Fox)
57158.2	328	34.30 ± 5.44	29.57 ± 5.61	11053 (Fox)

[a]Fluxes are in units of μJy. Uncertainties are statistical. Epochs are given as days from V-band peak (MJD 56830.3; Mauerhan et al. 2015).

3 RESULTS & ANALYSIS

The absolute-magnitude light curve of SN Hunt 248 is shown in Figure 4, including data from Mauerhan et al. (2015) and Kankare et al. (2015). At ~ 1 yr after the peak of the 2014 outburst, the source has dropped to a brightness of $V = 25.46 \pm 0.03$ mag, which is a factor of ~ 10 less luminous in the optical than the faintest pre-outburst state ever measured for the stellar precursor in the year 2005 ($V = 22.91 \pm 0.01$ mag; see Mauerhan et al. 2015). Yet, as illustrated in Figure 5, the $B - V$ colour of 0.38 ± 0.06 mag is consistent with no change from the precursor value of 0.39 ± 0.02 mag, while the $V - I$ colour of 0.95 ± 0.05 mag has become only slightly redder from the precursor value of 0.81 ± 0.01 mag.

The latest epoch of near-IR H and K photometry from Kankare et al. (2015) nearly coincides with our *HST* UV-optical data from days 369–374 and *Spitzer* mid-IR photometry from 325. We combined these data to construct a spectral energy distribution (SED) for the source, shown in Figure 6; the strong thermal-IR component of the SED is clearly seen.

3.1 Dust modeling

We analyze the *Spitzer* data using a simple dust model (Fox et al. 2011). We assume that the source of the mid-IR excess is warm dust, and fit the SED as a function of the dust mass ($M_{\rm d}$) and temperature ($T_{\rm d}$). The flux is given by (Hildebrand et al. 1983)

$$F_\nu = \frac{M_{\rm d} B_\nu(T_{\rm d}) \kappa_\nu(a)}{d^2}, \qquad (1)$$

where a is the dust grain radius, $\kappa_\nu(a)$ is the dust absorption coefficient, and d is the distance of the dust from the

[2] http://irsa.ipac.caltech.edu/data/SPITZER/docs/irac/iracinstrumenthandbook/27/

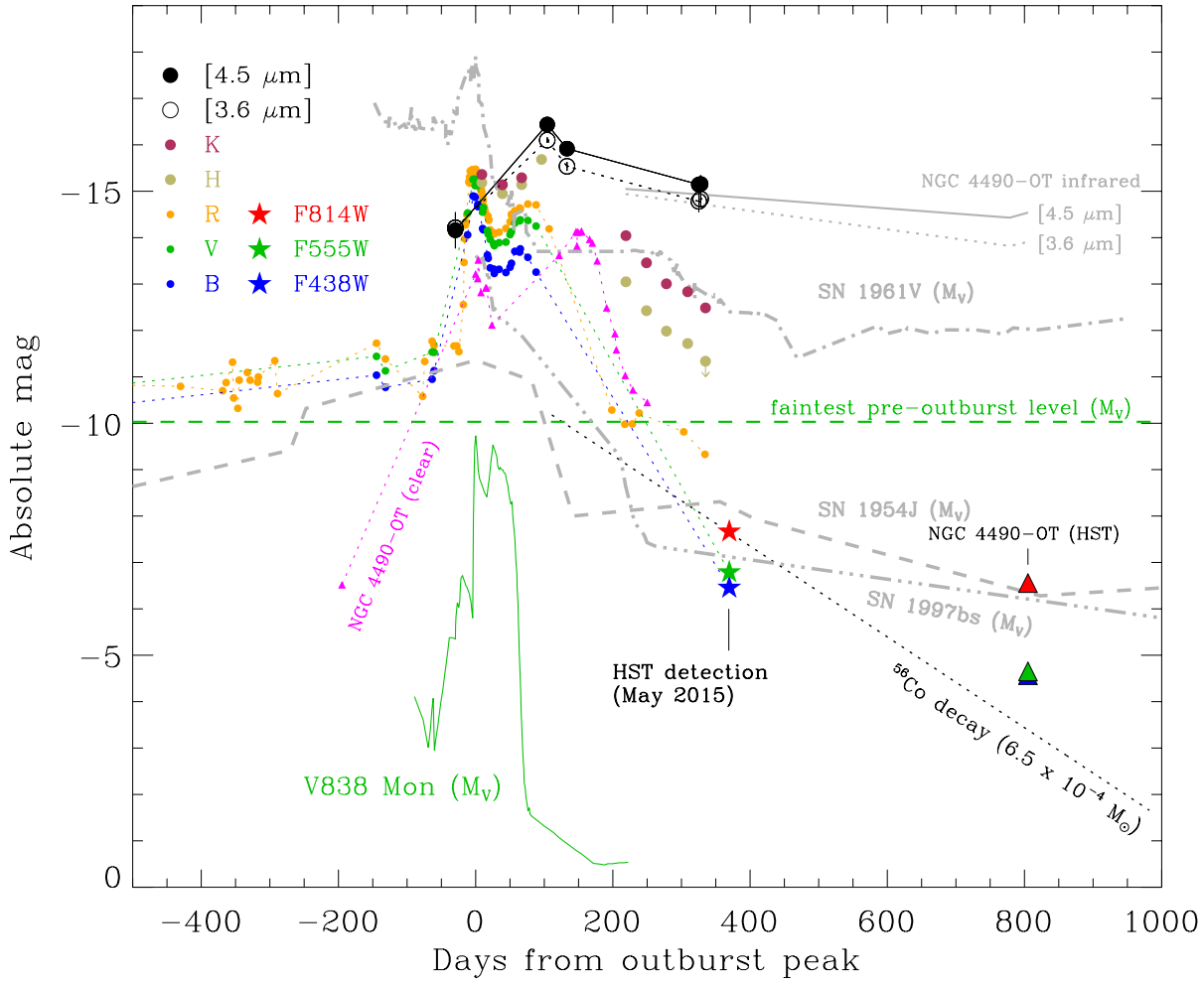

Figure 4. Long-term light curve of SN Hunt 248 (coloured filled circles), including the late-time mid-IR *Spitzer* (black open and filled circles) and UV-optical *HST* data (coloured 5-pointed stars) presented in this work. Optical and near-IR photometric data of the precursor and main outburst are from Mauerhan et al. (2015) and Kankare et al. (2015). The optical photometry of NGC 4490-OT is also shown as coloured triangles (magenta is ground-based clear-filter photometry; red, green, and blue are late-time F814W, F555W, and F438W filter photometry from *HST*; see Smith et al. 2016); mid-IR *Spitzer* data are shown as grey solid and dotted curves. The optical light curves of several SN impostors are displayed for comparison, including SN 1997bs (dashed triple-dotted grey curve; Van Dyk et al. 2000), SN 1961V (dot-dashed grey curve; see Smith et al. 2011 and references therein), and SN 1954J (dashed grey curve; Tammann & Sandage 1968). The green horizontal dashed line represents the faintest pre-outburst V-band absolute magnitude of the precursor star (see Mauerhan et al. 2015). For reference, the decline rate for 6.5×10^{-4} M$_\odot$ of radioactive ^{56}Co decay (with respect to the onset of outburst, but only displayed for $>$ 100 days post-outburst) is illustrated by the black dotted line; this mass value was chosen to match the F814W photometry of SN Hunt 248 from day 371.

Table 3. Dust model parameters for SN Hunt 248.

MJD	Epoch (days)	L (10^6 L$_\odot$)	M (10^{-5} M$_\odot$)	T (10^2 K)
56800.71	−30	< 2.0	< 2.1	< 15.4
56934.57	104	$3.1^{+0.9}_{-2.7}$	$2.7^{+0.5}_{-1.1}$	$8.7^{+1.2}_{-2.5}$
56963.38	133	$1.7^{+1.0}_{-0.3}$	$2.0^{+2.9}_{-1.2}$	$8.3^{+2.3}_{-1.4}$
57155.54	325	$0.9^{+2.3}_{-0.2}$	$0.9^{+3.8}_{-0.7}$	$8.5^{+5.6}_{-2.4}$
57158.19	328	$1.0^{+2.5}_{-0.3}$	$0.8^{+2.6}_{-0.6}$	$8.8^{+5.7}_{-2.3}$

Uncertainties are statistical. Epochs given in days with respect to V-band peak on MJD 56830.28 (Mauerhan et al. 2015).

observer. We assume $a = 0.1\,\mu$m and derive κ for graphite dust, following Fox et al. (2010). For silicates at this grain size, the value of κ in the wavelength range of interest is comparable to that of graphite (see Fox et al. 2010; their Figure 4), so the choice of graphite over silicates does not have a substantial affect on our results. For simplicity (and given the limited number of data points), we assume optically thin dust emitting at a single equilibrium temperature (e.g., Hildebrand et al. 1983). Table 3 lists the best-fitting parameters.

For our earliest epoch 30 days before peak of the 2014 eruption we obtain only upper limits for our dust model pa-

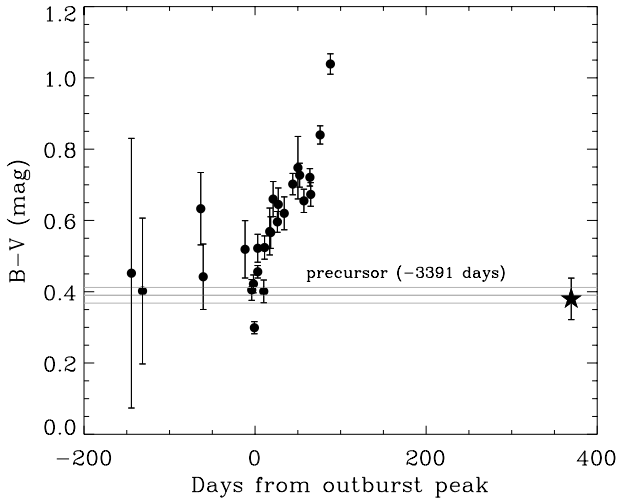

Figure 5. $B-V$ colour evolution of SN Hunt 248. The horizontal lines represent the value (thick line) and uncertainty envelope (thinner lines) of the stellar precursor detected with *HST* at −3391 days (see Mauerhan et al. 2015). Filled dots are data from Kankare et al. (2015). The filled 5-pointed star is our most recent measurement from Table 1, which exhibits the same value as the precursor from 3762 days prior.

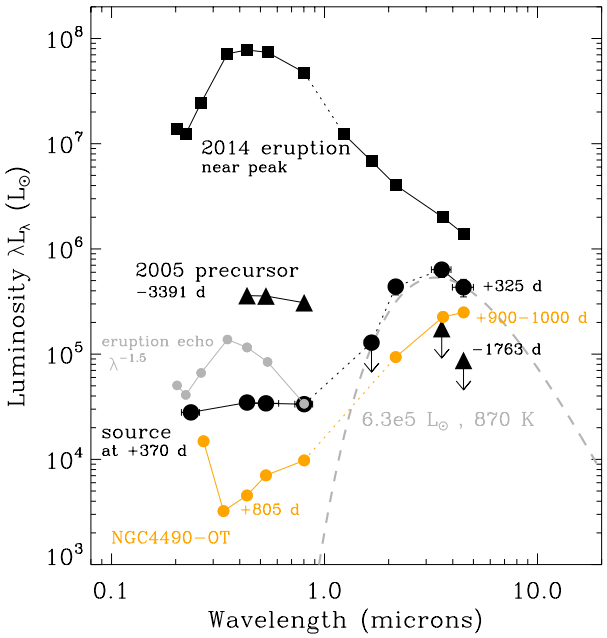

Figure 6. UV-IR SED of SN Hunt 248, including the faintest observed stellar precursor optical measurements from 2005 (black triangles) and *Spitzer* upper limits from −1763 days relative to eruption peak (black triangles with downward facing arrows), the 2014 outburst near peak (black squares), and the remnant in 2015 (black filled circles). The expected UV-optical SED of an echo from the 2014 eruption is shown (grey filled circles), scaled by $\lambda^{-1.5}$ and anchored to the I-band data of the remnant for comparison. A modified black body (λ^{-1} emissivity) with $T = 870\,\mathrm{K}$ and $L = 6.3\times10^5\,\mathrm{L}_\odot$ is represented by the dashed grey line. The UV-IR SED of massive stellar merger candidate NGC 4490-OT is also shown for comparison (orange filled circles; data from Smith et al. 2016, and reddened here by adopting their extinction estimate, $A_V = 0.06$ mag and the extinction relation of Cardelli, Clayton, & Mathis (1989).

rameters of interest. From 104 days after outburst peak out to day 328, we measure no significant change in the physical parameters of the dust. The dust appears to remain consistent with the hot $\sim 870\,\mathrm{K}$ temperature measured on day 104, and exhibits a luminosity $\sim 6.3\times10^5\,\mathrm{L}_\odot$. The inferred dust mass is $\sim 10^{-5}\,\mathrm{M}_\odot$. For a canonical dust-to-gas ratio of 1/100, this would imply a gas mass of $\sim 10^{-3}\,\mathrm{M}_\odot$. Of course, the dust-mass estimate should probably be regarded as a lower limit, since there might also be cooler dust to which our *Spitzer* observations at $3.6\,\mu$m and $4.5\,\mu$m are not sensitive.

4 DISCUSSION

4.1 The nature of the UV-optical remnant and its thermal counterpart

The SED of the UV-IR remnant of SN Hunt 248, shown in Figure 6, appears very similar to that of NGC 4490-OT (Smith et al. 2016). In both cases, the emitting dust is hot and the UV-optical counterpart exhibits noteworthy UV flux, especially NGC 4490-OT. Interestingly, the mid-IR brightness evolution of the remnants of SN Hunt 248 and NGC 4490-OT are very similar, as shown in Figures 4 and 6. and they both exhibit dust luminosities that are the same order of magnitude as their directly identified stellar precursors ($L_{\rm pre} \approx 4\times10^5\,\mathrm{L}_\odot$ in the case of SN Hunt 248; Mauerhan et al. 2015); taken at face value, this seems to be consistent with heating of the dust by the central stellar source.

If the UV-optical component of the SED is from a surviving star and the thermal emission is from newly synthesized dust that absorbs stellar radiation, then it is surprising that the dust is not effectively obscuring it or reddening the star's UV-optical SED. As demonstrated by the *HST* photometry, the $B-V$ colour of the remnant, shown in Figure 5, appears unchanged from the stellar precursor colour. One possible explanation for the apparent lack of reddening is that the absorbing dust grains could be larger than the $0.1\,\mu$m radius we assumed in our simple dust model, and closer to $1.0\,\mu$m, which would result in less attenuation of stellar light. This is the case in η Car's Homunculus nebula, which, although very dusty, is less effective at absorbing the UV-optical flux of the central star than in the case of smaller grains (Rodgers 1971; Smith 2010). For relatively large grains, the thermal dust emission might be more appropriately modeled by a modified black body (a "grey body"), where the emissivity of the dust is proportional to λ^{-1}. In fact, a grey-body form yields the best match to the IR component of the SED in Figure 6. The post-eruption UV-IR SED of the NGC 4490-OT, which appears similar to that of SN Hunt 248, was also shown to be consistent with such a grey-body dust component (in that case, optical colours were not available for the stellar precursor).

It is also possible that the post-eruption source is intrinsically much bluer than it appears, and was coincidentally reddened by dust back to a colour that is comparable to that of the stellar precursor. This possibility raises an interesting

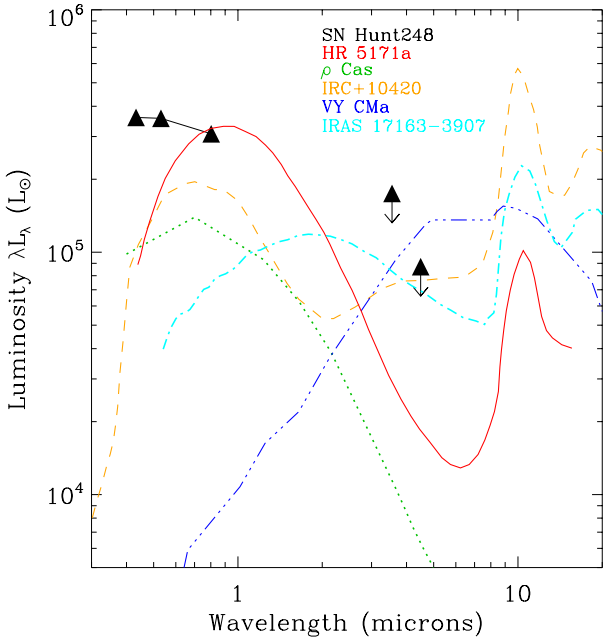

Figure 7. Optical luminosity of SN Hunt 248 (filled triangles; Mauerhan et al. 2015) and its mid-IR limits (black filled triangles with downward facing arrows) compared with literature-extracted SEDs for the Galactic cool-warm hypergiants VY CMa, ρ Cas, and IRC+10420 (blue dashed triple-dotted, green dotted, and orange dashed curves, respectively; Shenoy et al. 2016), HR5171a (red solid curve; Humphreys et al. 1971), and IRAS 17163−3907 (cyan dashed-dotted curve; Lagadec et al. 2011). The following distances were used to calculate luminosity: SN Hunt 248 (26.4 Mpc; Mauerhan et al. 2015), ρ Cas (2.5 kpc; Humphreys 1978); VY CMa (1.2 kpc; Shenoy et al. 2016), IRC+10420 (5 kpc; Shenoy et al. 2016), HR5171 (3.6 kpc; Chesneau et al. 2014), IRAS 17163−3907 (4.2 kpc, average of range estimate from Lagadec et al. 2011). The IRAS 17163−3907 data were corrected for interstellar extinction in this work, adopting $A_V = 2.1$ mag (Lagadec et al. 2011) and the extinction relation of Cardelli, Clayton, & Mathis (1989). The other SEDs from the literature account for interstellar extinction only.

question: could the 2014 eruption have cleared out the cool-hypergiant pseudophotosphere discussed by Mauerhan et al. (2015), revealing a hotter star lying underneath? Another explanation for the lack of UV-optical attenuation could be that the emitting dust is distributed in an aspherical configuration that does not effectively obscure the star along our line of sight; this possibility is interesting in the context of the stellar-merger hypothesis discussed in the next section.

We must also address the possibility that the post-outburst IR excess is the result of pre-existing circumstellar dust that was shock heated as the fast outflow from the 2014 eruption overran the slow CSM from the cool-hypergiant precursor. Unfortunately, our *Spitzer* mid-IR upper limits on the stellar precursor are not sufficiently deep to provide a meaningful constraint on the pre-existing dust mass, or to tell if the dust mass was lower before the eruption. For example, in Figure 7, we show the SED of SN Hunt 248 along with those of several Galactic cool hypergiants that have measured circumstellar dust masses in the literature. Our limits are mutually consistent with a system like ρ Cas, which has a rather low estimated dust mass of $\sim 3 \times 10^{-8}\,M_\odot$ (Jura & Kleinmann 1990) and more extreme dusty systems, like IRC+10420 (Shenoy et al. 2016) and IRAS 17163−3907 (Lagadec et al. 2011), the latter of which has a much larger dust mass of $\sim 0.04\,M_\odot$. The comparison in Figure 7 does, however, suggest that the IR excess from a system such as VY CMa, with a total dust mass of $\sim 0.02\,M_\odot$ (Harwit et al. 2001; Muller et al. 2007), would have been detectable with our photometry at 4.5 μm. We conclude that the $\sim 10^{-5}\,M_\odot$ dust mass we inferred *post* eruption could have been pre-existing yet not detectable by our *Spitzer* observations. Again, however, the relatively high brightness of the optical precursor star in the B and V bands, when compared to the other hypergiants in (Figure 7), would suggest that the stellar precursor of SN Hunt248 did not suffer a comparable level of attenuation by circumstellar dust.

A light echo of the 2014 eruption off of outer dusty CSM is another potential contributor to the source flux at late times, which could result in delayed scattering of UV-optical light and thermal reprocessing of the fraction of light that gets absorbed by the dust. However, assuming that such an echo is dominated by light from the peak of the outburst and obeys a $\propto \lambda^{-1.5}$ wavelength dependence (e.g., see Fox et al. 2015), while suffering the same extinction as the precursor, the expected UV-optical SED is totally inconsistent with the observed SED at +370 days (see Figure 6). The thermal-IR remnant also appears to be inconsistent with thermal reprocessing of an echo, as the dust temperature requires a luminosity that is far above the peak of the 2014 event. This was determined using the same line of reasoning invoked for the analysis of the remnant of NGC 4490-OT (see Smith et al. 2016, their §3.2.3). Assuming the ratio of the efficiencies of UV absorption to IR emission $Q_{\rm UV}/Q_{\rm IR} = 0.3$ (Smith et al. 2016), the luminosity required to heat dust at a distance r to a temperature T can be expressed as $L/L_\odot \approx 5.7 \times 10^{12}\,(T_d/1000\,{\rm K})^4\,(r/{\rm pc})^2$. At 328 days the minimum distance of the echo-heated dust is $r \approx 0.3$ pc. Thus, the range of possible dust temperatures inferred from our model (650–1450 K) requires a peak outburst luminosity in the range (1–25) $\times 10^{11}\,L_\odot$, which is at least 3 orders of magnitude higher than the observed peak of the 2014 outburst. Furthermore, the temperature evolution of a thermally reprocessed echo is given by $T \propto t^{-0.5}$ (Fox et al. 2011, 2015), and so we would have expected the temperature between 133 days and 325 days to have dropped from ~ 830 K to ~ 60 K; instead, the temperature evolution is consistent with no change between these epochs. We therefore conclude that a light echo is probably not the source of the late-time UV-optical source and its thermal counterpart.

Finally, it is possible that the the UV-optical flux of the point source is not from the same star that generated the 2014 outburst, and is a nearby star, star cluster, or a companion to the eruptive source. Future epochs of multi-wavelength photometry will be necessary to test this possibility; if the UV-optical flux is dominated by separate neighbouring stellar sources, then we expect no significant change with time.

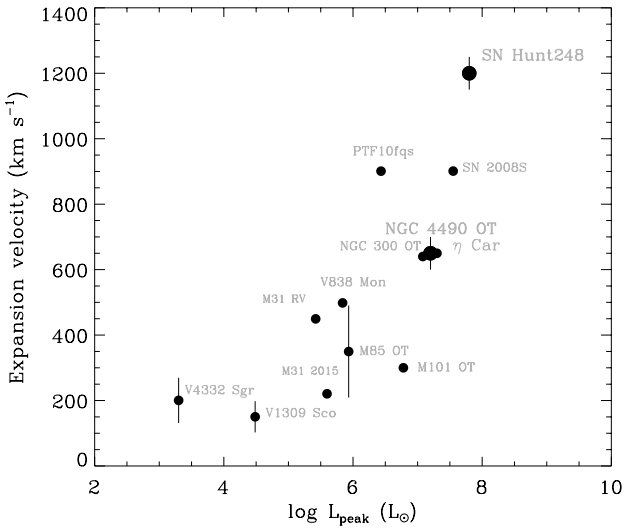

Figure 8. Peak outburst luminosity versus outflow velocity for SN Hunt 248 and other stellar merger candidates, including NGC 4490-OT (Smith et al. 2015) and the sample presented by Pejcha et al. (2016a, their Figure 21). η Car is also included. Uncertainties in expansion velocity are included where available.

4.2 The 2014 outburst, revisited

4.2.1 Massive binary merger burst?

The energy source of the 2014 eruption is uncertain. The structure of the outburst light curve, the outflow velocity, and the large-amplitude pre-outburst variability detected for decades prior might provide clues. We speculate that the cool-hypergiant precursor was a massive interacting binary. Could SN Hunt 248's 2014 event have been a merger burst marking the coalescence of two massive stars? Such event might be more common than previously thought (Kochanek 2014). The merger hypothesis was invoked as the favoured interpretation of NGC 4490-OT (Smith et al. 2016), whose remnant SED during a similar phase appears very similar to that of SN Hunt 248, and whose light curve also exhibited a multi-peaked structure.

Figure 8 shows the peak outburst luminosity versus outflow velocity[3] for SN Hunt 248 (Mauerhan et al. 2015); NGC 4490-OT (Smith et al. 2016); the sample of merger candidates presented in Pejcha et al. (2016a; their Figure 21); M101-OT, also considered a merger candidate or binary common-envelope ejection event (Blagorodnova et al. 2017); and η Car (Smith et al. 2003; Smith & Frew 2011). Interestingly, SN Hunt 248 is consistent with the apparent trend exhibited by this sample of merger candidates. V1309 Sco was almost certainly a true merger, based on the exquisite light curve that showed the rapidly decreasing orbital period of an inspiraling binary. Both V1309 Sco and V838 Mon exhibited a double-peaked light curves, of shorter duration and brightness than SN Hunt 248 and NGC 4490-OT, but similar in multi-peaked morphology. Smith et al. (2016) interpreted NGC 4490-OT as a stellar merger involving stars of relatively high mass, and reiterated the suggestion that η Car's historic eruption was the result of a massive merger. η Car's position in Figure 8 also fits in with the apparent trend exhibited by other merger candidates.

A double-peaked light curve might be a natural consequence of a stellar merger burst that follows a common-envelope phase. A close binary of evolved massive stars that are headed for a merger will experience mass transfer, and this can occur even if the primary radius does not fully fill its Roche lobe, but fills it up with material from a slow wind (e.g., wind Roche-lobe overflow, WRLOF; Abate et al. 2013). RLOF may be nonconservative and WRLOF is nonconservative by nature (i.e., some mass is lost rather than exchanged). The process leads to the buildup of CSM that is concentrated in the equatorial plane of the binary, perhaps forming a spiral pattern (Pejcha et al. 2016a, 2016b). The outflow velocity through the outer Lagrange points is proportional to the orbital velocity of the stars. Thus, as the orbital period of the inspiraling stars decreases and the orbital velocity increases, the outflow velocity will increase as well, leading to a pileup of gas with a toroidally enhanced distribution (e.g., Ohlmann et al. 2016). The subsequent explosive outflow from a merger burst will encounter the toroidal CSM distribution and generate radiation from the resulting interaction (a second peak in the light curve). Any interaction-induced dust formation will mirror the geometry of the pre-existing CSM. Interestingly, The circumstellar environment of the purported post-merger system V838 Mon exhibits an equatorial overdensity of dust several hundred AU in extent (Chesneau et al. 2014b). Hydrodynamic simulations have also shown that equatorially enhanced dust formation should be expected in the aftermath of mergers (Pejcha et al. 2016a). If SN Hunt 248 was the result of a stellar merger, then the outflow from the previously interacting binary system is likely to be concentrated in the equatorial plane, and any dust formation in the cooling ejecta could exhibit a similar geometry. Therefore, if a post-merger system is suitably inclined, our line of sight to the stellar remnant could be relatively free of obscuring dust. This is one possible explanation for why the UV-optical remnants of SN Hunt 248 and NGC 4490-OT appear to be free of the heavy attenuation that has been associated with many other massive stars after their outbursts (e.g., Adams et al. 2016; Kochanek et al. 2012).

4.2.2 Failed supernova?

The so-called red supergiant (RSG) problem refers to the statistically significant lack of nearby core-collapse supernovae (SNe) of Type II-P stemming from directly identified progenitors with stellar masses in the range 16–30 M$_\odot$ (Smartt et al. 2009). It could be that stars within this mass range might lose their massive hydrogen envelopes to giant super-Eddington eruptions (whatever their cause), and thus do not end their lives with the production of normal Type II-P SNe (Yoon & Cantiello 2010), as RSGs of lower mass do. The estimated initial mass of SN Hunt 248 is $\sim 30\,M_\odot$ and the 2014 eruption was indeed super-Eddington (Mauer-

[3] We note that the outflow velocities of SN Hunt 248 and NGC4490-OT were measured from their P-Cygni absorption minima (Mauerhan et al. 2015; Smith et al. 2016), whereas the outflow velocities of the sample in Pecha et al. (2016a) were measured mostly by Hα line widths, and η Car's velocity measurement is from detailed spectroscopic analysis of the Homunculus nebula (Smith et al. 2003).

han et al. 2015), so SN Hunt 248 might be relevant in this context. Interestingly, it has been suggested that stars with initial masses near $30\,M_\odot$ might not be successful at producing bright explosions when their cores collapse, instead producing weak fallback SNe or direct collapse to a black hole, either of which might result in very faint or undetectable emission from radioactive decay (Woosley & Heger 2012; Lovegrove & Woosley 2013; Kochanek et al. 2008, 2014; Clausen et al. 2015). Thus, it is also worth speculating on the possibility of a weak or failed SN as the source of the 2014 eruption of SN Hunt 248. In Figure 4 we showed that the latest optical photometry limits the synthesized mass of radioactive ^{56}Ni to $< 6.5 \times 10^{-4}\,M_\odot$. Interestingly, the prototype SN impostor SN 1997bs (Van Dyk et al. 2000) exhibited an optical remnant of comparable brightness to SN Hunt 248 at $\sim$1 yr after its peak, that continued to fade during subsequent coverage (Kochanek et al. 2012). Adams & Kochanek (2015) recently showed that the optical-IR remnant of SN 1997bs now appears to be consistent with a weak but terminal explosion, as few plausible combinations of obscuring dust and surviving stellar luminosity can explain the characteristics of the present source. Could SN Hunt 248 have suffered a similar fate? If so, this would imply that the late-time optical emission, if truly associated with the outbursting source, could be powered by continued shock interaction of an otherwise weak or failed core explosion.

5 CONCLUDING REMARKS

Based on the late-time photometry of the UV-optical and mid-IR source at the position of SN Hunt 248, all we can state with confidence is that, as of June 2015, the optical brightness is over a factor of 10 less than the faintest pre-outburst level for the stellar precursor, and that there is a thermal counterpart of hot dust with a mass $> 10^{-5}\,M_\odot$ that was probably synthesized in the aftermath of the 2014 eruption. The luminosity of the thermal dust emission is comparable to the optical luminosity of the hypergiant precursor and thus seems consistent with the absorption of radiation from a surviving stellar source. However, the UV-optical colour of the late-time source appears inconsistent with significant attenuation by dust. Whether the UV-optical source is a separate star or cluster, a surviving star from a super-Eddington eruption, the byproduct of a massive stellar merger (see §4.2.1), or the decaying emission from a terminal event, will be elucidated with future UV through IR monitoring of the source using *HST* and the *James Webb Space Telescope*. In particular, an additional epoch of data to track the evolution of the UV-IR SED will allow for the construction of more complex models involving a surviving central source attenuated by an evolving dust component.

ACKNOWLEDGEMENTS

This work is based in part on observations made with the NASA/ESA *Hubble Space Telescope*, obtained from the Data Archive at the Space Telescope Science Institute (STScI), which is operated by the Association of Universities for Research in Astronomy (AURA), Inc., under NASA contract NAS5-26555. It is also based in part on observations and archival data obtained with the *Spitzer Space Telescope*, which is operated by the Jet Propulsion Laboratory, California Institute of Technology, under a contract with NASA; support was provided by NASA through an award issued by JPL/Caltech. A.V.F.'s group at U.C. Berkeley is also supported by Gary & Cynthia Bengier, the Richard & Rhoda Goldman Fund, the Christopher R. Redlich Fund, and the TABASGO Foundation.

REFERENCES

Abate, C., Pols, O. R., Izzard, R. G., Mohamed, S. S., & de Mink, S. E. 2013, A&A, 552, A26
Adams, S. M., & Kochanek, C. S. 2015, MNRAS, 452, 2195
Adams, S. M., Kochanek, C. S., Prieto, J. L., et al. 2016, MNRAS, 460, 1645
Blagorodnova, N., Kotak, R., Polshaw, J., et al. 2017, ApJ, 834, 107
Chesneau, O., Meilland, A., Chapellier, E., et al. 2014a, A&A, 563, A71
Chesneau, O., Millour, F., De Marco, O., et al. 2014b, A&A, 569, L3
Clausen, D., Piro, A. L., & Ott, C. D. 2015, ApJ, 799, 190
Cardelli, J. A., Clayton, G. C., & Mathis, J. S. 1989, ApJ, 345, 245
Dolphin, A. E. 2000, PASP, 112, 1383
Fox, O. D., Chevalier, R. A., Dwek, E., et al. 2010, ApJ, 725, 1768
Fox, O. D., Chevalier, R. A., Skrutskie, M. F., et al. 2011, ApJ, 741, 7
Fox, O. D., Smith, N., Ammons, S. M., et al. 2015, MNRAS, 454, 4366
Hildebrand, R. H. 1983, QJRAS, 24, 267
Humphreys, R. M. 1978, ApJS, 38, 309
Humphreys, R. M., Strecker, D. W., & Ney, E. P. 1971, ApJL, 167, L35
Jura, M., & Kleinmann, S. G. 1990, ApJ, 351, 583
Kankare, E., Kotak, R., Pastorello, A., et al. 2015, A&A, 581, L4
Kochanek, C. S. 2014, ApJ, 785, 28
Kochanek, C. S., Adams, S. M., & Belczynski, K. 2014, MNRAS, 443, 1319
Kochanek, C. S., Beacom, J. F., Kistler, M. D., et al. 2008, ApJ, 684, 1336
Kochanek, C. S., Szczygieł, D. M., & Stanek, K. Z. 2012, ApJ, 758, 142
Lagadec, E., Zijlstra, A. A., Oudmaijer, R. D., et al. 2011, A&A, 534, L10
Lovegrove, E., & Woosley, S. E. 2013, ApJ, 769, 109
Mauerhan, J. C., Van Dyk, S. D., Graham, M. L., et al. 2015, MNRAS, 447, 1922
Ohlmann, S. T., Röpke, F. K., Pakmor, R., & Springel, V. 2016, ApJL, 816, L9
Pejcha, O., Metzger, B. D., & Tomida, K. 2016a, MNRAS, 455, 4351
Pejcha, O., Metzger, B. D., & Tomida, K. 2016b, MNRAS, 461, 2527
Rodgers, A. W. 1971, ApJ, 165, 665
Shenoy, D., Humphreys, R. M., Jones, T. J., et al. 2016, AJ, 151, 51
Shiode, J. H., & Quataert, E. 2014, ApJ, 780, 96
Smartt, S. J., Eldridge, J. J., Crockett, R. M., & Maund, J. R. 2009, MNRAS, 395, 1409
Smith, N. 2010, MNRAS, 402, 145
Smith, N. 2014, ARA&A, 52, 487
Smith, N., Andrews, J. E., Van Dyk, S. D., et al. 2016, MNRAS, 458, 950
Smith, N., & Arnett, W. D. 2014, ApJ, 785, 82
Smith, N., & Frew, D. J. 2011, MNRAS, 415, 2009
Smith, N., Li, W., Silverman, J. M., Ganeshalingam, M., & Filippenko, A. V. 2011, MNRAS, 415, 773
Smith, N., & Tombleson, R. 2015, MNRAS, 447, 598
Smith, N., Vink, J. S., & de Koter, A. 2004, ApJ, 615, 475
Smith, N., Gehrz, R. D., Hinz, P. M., et al. 2003, AJ, 125, 1458
Tammann, G. A., & Sandage, A. 1968, ApJ, 151, 825
Van Dyk, S. D., & Matheson, T. 2012, ApJ, 746, 179
Van Dyk S. D., Peng C. Y., King J. Y., et al. 2000, PASP, 112, 1532
Woosley, S. E., & Heger, A. 2012, ApJ, 752, 32
Yoon, S.-C., & Cantiello, M. 2010, ApJL, 717, L62